Desalination and Water Treatment
www.deswater.com

doi: 10.5004/dwt.2021.27649

234 (2021) 299–308
September

Degradation of refractory organics in pre-coagulated leachate concentrate using the Fenton process: optimization through response surface methodology

Wenqiang Wang*, Aili Wang, Fang Wang, Shubo Shang, Chunhui Li

College of Chemistry and Chemical Engineering, Dezhou University, Dezhou 253023, China, Tel./Fax: +86 534 8987866; emails: wwqzs@126.com (W. Wang), sxz_li@126.com (A. Wang), wf0085@126.com (F. Wang), shangshubobo@163.com (S. Shang), lichunhui-tj@163.com (C. Li)

Received 3 March 2021; Accepted 20 July 2021

ABSTRACT

Membrane separation technology is widely used in the treatment of landfill leachate, which inevitably produces a large amount of leachate concentrate (LC). High concentrations of refractory organics must be removed from LC to prevent harm to the environment. In this study, the Fenton process was performed and optimized using response surface methodology to remove refractory organics from pre-coagulated leachate concentrate (PCLC), and the highest chemical oxygen demand (COD), total organic carbon, color number, and ultraviolet absorbance at 254 nm (UV_{254}) removal efficiencies were 57.40%, 53.47%, 83.03%, and 64.59%, respectively, under optimal conditions of a pH of 2, H_2O_2 concentration of 0.7 mol/L, and Fe^{2+} concentration of 7.2 mmol/L. The COD concentration in the PCLC was reduced from 676 to 288 mg/L. The statistical analysis showed satisfaction of the obtained regression model for COD removal efficiency, and that H_2O_2 had the greatest effect. The biodegradability of the Fenton effluent was improved, and the aromatic degree and complexity of coagulation-resistant organic substances were reduced by the Fenton process. Fourier transform infrared and spectrophotometric analyses showed that the majority of organic matter was fulvic acid and humic acid, which were effectively removed during the Fenton process. The increasing biodegradability, the 5-day biochemical oxygen demand (BOD_5)/COD ratio rising from 0.13 to 0.26, enabled the Fenton oxidation process to provide the possibility for subsequent biological treatment of the concentrate.

Keywords: Pre-coagulated leachate concentrate; Fenton process; Refractory organics; Response surface methodology

1. Introduction

Landfill leachate generated in sanitary landfills owing to rainwater percolation, physicochemical interactions, and organics biodegradation contains refractory organic matters and poses hazards to the environment and human health in the absence of appropriate treatment [1]. In order to meet stricter Chinese discharge criteria (GB 16889-2008), membrane separation processes such as reverse osmosis (RO) and nanofiltration have been used in further treatment of landfill leachate after aerobic–anaerobic processes owing to the high efficiency for removal of pollutants and low energy consumption compared with conventional strategies [2,3]. Leachate concentrate (LC), typically accounting for 15%–30% of the raw leachate, is inevitably generated by membrane filtration and characterized by extremely low biodegradability and high concentrations of recalcitrant organic matters, inorganic salts, and heavy metals. The toxicity of LC to organisms has been confirmed by luminescent bacteria [4]. Therefore, the development of an economical and effective method for the treatment of LC is a challenge.

Physicochemical methods are particularly suitable for the treatment of wastewater with very low biodegradability due to the presence of large amounts of refractory organic

---

* Corresponding author.

matter, such as LC [5]. Apart from recirculation [6], solidification/stabilization [7], evaporation [8], and coagulation [9], advanced oxidation processes (AOPs) are the most common methods for oxidizing recalcitrant organics in LC and improving the potential for follow-up biological treatment of the resulting effluent at the expense of high chemical dosage and high energy demand. Among the AOPs, the Fenton process is relatively inexpensive, efficient, simple, and provides good degradation of refractory pollutants [10]. Fenton and other AOPs treatment of LC have been conducted by some researchers [11–16]. The chemical oxygen demand (COD) of 90%, the color of 96.5%, and ultraviolet absorbance at 254 nm (UV_{254}) of 97.2% were removed from the raw LC, respectively, by the Fenton process which was optimized using response surface methodology (RSM), and the biodegradability was improved, increasing the 5-day biochemical oxygen demand (BOD_5)/COD ratio from the value of 0.04 to the value of 0.4 [11]. When microwave irradiation was introduced into the Fenton oxidation, a comparative COD, UV_{254}, and the color number (CN) removal rate of 75%, 83%, and 95%, and a high BOD_5/COD of 0.62 was achieved under an extremely shortened reaction time of only 8 min and a microwave power of 390 W [12]. A photo-Fenton process increased the ratio between the BOD_5 and the COD from 0.06 to 0.4, resulting in an enhanced biodegradability, and an extra 43% of the COD was removed from the coagulated landfill leachate RO concentrate [13]. RSM was applied to optimize the electro-Fenton system to treat the high ammonia nitrogen (NH_3–N) landfill leachate nanofiltration concentrate, and COD removal rate of 77.24% and NH_3–N removal rate of 74.62% was achieved [14]. A combined heat/UV activated persulfate process was used to treat the nanofiltration concentrated leachate, and the maximum rate of COD, NH_3–N and UV_{254} removal were 65.4%, 51.4% and 98.1%, respectively, at a persulfate concentration of 18 g/L, initial solution pH before the reaction of 9.0, UV lamp power of 60 W and temperature of 80°C [15]. For the concentrated leachate treatment using the Fe^{2+} catalyzed O_3/H_2O_2 process, the COD and UV_{254} removal efficiencies under the optimal conditions were 48.82% and 63.59%, respectively [16]. It can be seen that the Fenton process and other AOPs have comparable treatment effects, but the former does not require additional energy input or special reactors which is an alternative treatment method. One of the effective, economical pretreatment methods for LC is coagulation, but it does not completely remove all organics from the concentrate [17]. In this study, considering the low pH value of the coagulation effluent and the remaining refractory compounds in the LC, the Fenton process was employed to remove refractory organics from pre-coagulated leachate concentrate (PCLC).

To reduce the expense of high chemical dosage, the Fenton process requires optimized conditions (e.g., pH, H_2O_2 and Fe^{2+} dosages) to achieve the best removal of refractory organics from LC. RSM is a widely used statistical method for experimental design, evaluation of individual and interaction effects of independent variables, and optimization of process parameters with a limited number of experiments [18]. RSM uses an experimental design, such as the Box–Behnken design (BBD), to identify the optimum conditions for a multivariable system [19]. The adequacy of the quadratic regression model is then determined by analysis of variance (ANOVA).

Currently, very few studies have used statistical methods to optimize the Fenton process for the treatment of LC and to investigate in detail the mechanism of degradation of refractory organics [20]. The objective of this study was to investigate the application of the optimized Fenton process by RSM based on the BBD to remove refractory organics from PCLC, to evaluate the single and interaction effects of the selected variables, that is, initial pH and the dosages of Fe^{2+} and H_2O_2, on the efficiencies of the process, and to propose a quadratic regression model by ANOVA to describe the quantitative relationship between the COD removal efficiency and the operating variables. Additionally, this study aimed to investigate the changes in the composition of organic substances before and after Fenton treatment to understand the mechanism of degradation of coagulation-resistant organics in the PCLC to improve the organic degradation of the Fenton process.

2. Materials and methods

2.1. Leachate concentrate

The LC samples used in this study were provided by a solid waste landfill plant located in China. The landfill has been in operation for 10 y. An anoxic/anoxic membrane bioreactor-RO hybrid process was employed to treat LC. The collected LC was stored at 4°C before the experiments were performed. The pretreated LC by coagulation at a pH of 5, $FeCl_3$ concentration of 1.4 g/L, and polyacrylamide concentration of 2 mg/L were further treated using the Fenton process. The characteristic properties of the LC, PCLC, and Fenton effluent are listed in Table 1.

2.2. Experimental methods

2.2.1. Fenton process

Fenton oxidation experiments of the PCLC were conducted in beakers using a six-paddle stirrer at ambient

Table 1
Characteristics of the LC, PCLC, and Fenton effluent

Parameter	pH	COD (mg/L)	BOD_5 (mg/L)	BOD_5/ COD	UV_{254} (cm^{-1})	CN (cm^{-1})	TOC (mg/L)	Conductivity (ms/cm)	TDS (g/L)
LC	7.4	1,240	113.80	0.09	18.816	0.4538	452	68.88	57.90
PCLC	5.0	676	90.00	0.13	4.405	0.2245	303	69.02	68.84
Fenton effluent	9.0	288	75.45	0.26	1.560	0.0381	141	75.55	75.40

COD, chemical oxygen demand; BOD_5, 5-day biochemical oxygen demand; TOC, total organic carbon; TDS, total dissolved solids.

temperature (20°C–25°C), which had no significant effect on the removal of organics in the Fenton treatment [21]. The operational reaction parameters of pH and Fe^{2+} and H_2O_2 dosages were optimized using RSM. First, the different initial pH value of the 100 mL PCLC was obtained using H_2SO_4 or NaOH. H_2O_2 and $FeSO_4·7H_2O$ were then added sequentially to reach the various target concentrations. To simplify the independent variables to be optimized for the Fenton process, the reaction time was set to 3 h which can ensure that Fenton oxidation is completed [20]. After 3 h of reaction, the pH of the resulting solution was adjusted to approximately 9 using 40% NaOH to induce precipitation and heated in a water bath at 50°C for 30 min to eliminate the influence of the residual H_2O_2 on the determination of an organic matter and finally left for 3 h. The collected supernatant was used for analysis. All experiments were performed twice and the average values were reported.

2.2.2. Experimental design

In order to optimize the Fenton process using RSM, single-factor experiments were conducted first to determine the main independent variables of the process and the range of values of the independent variables, and then the BBD experimental design was used to design the experimental conditions, and the experiments were conducted according to the designed experimental conditions. The data of the obtained response values, that is, COD removal efficiencies were substituted into the software, and the quantitative relationship equation between the independent variables and the response values was given by the software to complete the optimization of the Fenton process.

The experimental design and ANOVA were performed using the software Design-Expert 8.0 (Stat-Ease Inc., Minneapolis, USA). The correlation coefficient (R^2) was used to check the quality of the polynomial fitting model, a Student's *t*-test was employed to test its statistical significance, and *p* (probability) values were used to evaluate the model terms at a 95% confidence interval. When the theoretically calculated data of the model agreed well with the experimental data, a high R^2, which should be greater than 0.8 for a reasonable model, could be obtained. The predicted and adjusted determination coefficients should be reasonably consistent. A model with a coefficient of variation (CV) value below 10% was considered to be reasonably reproducible. The results of the ANOVA for the obtained model may help in determining whether the model is significant and evaluating the significance of each factor.

The relationship between the independent variables and responses is shown by the following quadratic model:

$$Y = b_0 + \sum_{i=1}^{k} b_i X_i + \sum_{i=1}^{k} b_{ii} X_i^2 + \sum_{i=1}^{k} \sum_{j=1}^{k} b_{ij} X_i X_j \quad (1)$$

where Y (COD removal efficiency) is the dependent variable; X_i is the independent variables (X_1 = pH; X_2 = [H_2O_2]; X_3 = [Fe^{2+}]); b_0 is the constant coefficient; b_i, b_{ii}, and b_{ij} are the corresponding regression coefficients; and k is the number of independent variables.

2.3. Analytical methods

The COD, total dissolved solids (TDS) and BOD_5 were determined using standard methods [22]. Total organic carbon (TOC) concentrations were measured using a Shimadzu TOC-VCPH analyzer. The CN was calculated according to Tizaoui et al. [23]. The samples were filtered through a 0.45 μm glass fiber membrane and UV_{254} was measured at 254 nm using an ultraviolet-visible (UV-Vis) spectrophotometer (JH752, Jinghua, China). Conductivity was measured using a conductivity meter (DDSJ-308F, Rex, China). The pH was determined using a pH meter (PHS-3C, Rex, China). Before and after optimal Fenton oxidation, the samples were used for Fourier transform infrared (FT-IR) measurement (Nicolet iS50, Thermo, USA) [24]. The samples were also used for absorbance scanning using a Shimadzu UV-2450 spectrophotometer (Shimadzu, Kyoto, Japan) and fluorescence excitation-emission matrix (EEM) spectra analysis by a fluorescence spectrophotometer (FLS980, Edinburgh, UK) after they were diluted 5 and 10 times to avoid errors associated with the inner filter effect [25], respectively. More details on these measurements were described in our previous work [17]. The EEM data analysis and identification of compounds based on specific peaks were performed by Origin 8.0 (Origin Lab Inc., USA) software.

3. Results and discussion

3.1. Preliminary Fenton experiments

3.1.1. Effect of pH

pH is one of the main factors limiting the performance of the Fenton process, which can control the activity of the stability of H_2O_2, the oxidant and organic matter, and the speciation of iron [21]. The pH conditions under which the Fenton reaction usually occurs depend on the quality of the wastewater, typically in the pH range of 2–5 [26]. The effect of pH on Fenton treatment of the PCLC with 7.2 mmol/L of $FeSO_4$ and 0.5 mol/L of H_2O_2 was studied in the pH range of 2–6. The results are presented in Fig. 1. As shown in Fig. 1, the COD removal efficiencies first increased and then decreased or lightly fluctuated with increasing

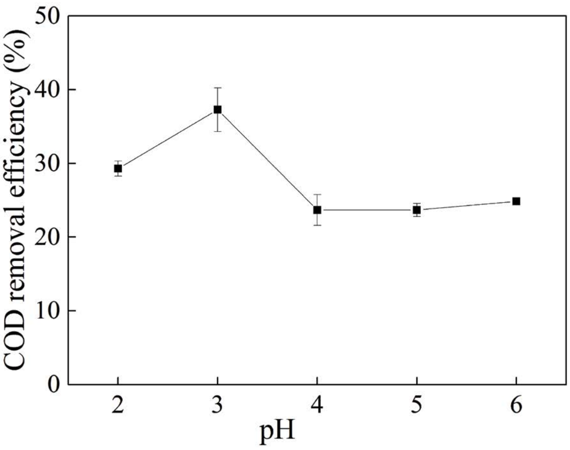

Fig. 1. Effect of pH on the COD removal efficiency.

pH, and the optimal pH value was 3 in terms of the COD removal efficiency. In acidic conditions (pH = 2–3), the generation of the large amount of $HO^•$ (hydroxyl radicals) [27], the limited $HO^•$ scavenging activity owing to the removal of inorganic carbon [28], and the increased solubility of iron improved the COD removal efficiency of the process [29]. Scavenging effect of high concentrations of hydrogen ions on $HO^•$ ($HO^• + H^+ + e^- \rightarrow H_2O$) resulted in the lower COD removal efficiency at pH = 2 than that at pH = 3 [30]. As the pH increased, the iron precipitated as $Fe(OH)_3$ and H_2O_2 was decomposed to oxygen, thereby reducing the COD removal efficiency [31].

3.1.2. Effect of H_2O_2 dosage

For the Fenton reaction, the concentration of H_2O_2 had a key effect on the COD removal from the PCLC. The results are presented in Fig. 2. Increasing the amount of H_2O_2 from 0.1 to 0.4 mol/L resulted in an increase in the initial removal rate of COD. Ultimately, the extent of COD removal ranged from 23.08% to 47.93%, which stemmed from significantly more $HO^•$ with the addition of H_2O_2. When H_2O_2 was increased from 0.4 to 0.5 mol/L, which resulted in the reduction of the oxidation efficiency, the removal rate of COD decreased from 47.93% to 39.64%. This was because a higher dosage of H_2O_2 may scavenge hydroxyl radical to produce hydroperoxyl radicals ($HO_2^•$) ($HO^• + H_2O_2 \rightarrow HO_2^• + H_2O$) with weaker reactivity for the degradation of organic contaminants [32,33]. Moreover, self-decomposition of H_2O_2 may also result in a reduction in the COD removal rate. Thus, 0.4 mol/L of H_2O_2 was an appropriate dosage based on its higher COD removal.

3.1.3. Effect of $FeSO_4$ dosage

Fig. 3 shows the effect of $FeSO_4$ dosage on the removal rate of COD at a pH of 3 and H_2O_2 concentration of 0.4 mol/L. The removal of COD initially increased as the $FeSO_4$ dose increased, but then decreased as the $FeSO_4$ dose increased from 7.2 to 10.8 mmol/L. When Fe^{2+} is overdosed, excessive Fe^{2+} could scavenge hydroxyl radical via reaction ($HO^• + Fe^{2+} \rightarrow Fe^{3+} + OH^-$), thus reducing the oxidation efficiency [34,35]. The best removal efficiency of COD was 51.85% at a $FeSO_4$ dosage of 7.2 mmol/L.

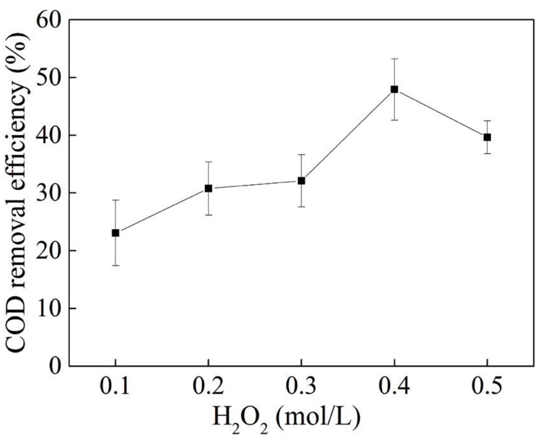

Fig. 2. Effect of H_2O_2 dosage on the COD removal efficiency.

3.1.4. Effect of reaction time

To investigate the effect of reaction time on the removal of the refractory organics by the Fenton oxidation, reaction times of 1, 3, 5, 8, and 12 h were tested. As shown in Fig. 4, with an increase in reaction time from 1 h to 3 h, the removal efficiency of COD increased rapidly from 28.40% to 48.59%. After a reaction time of 3 h, longer reaction times did not significantly increase COD removal. The reaction time for the Fenton process in various studies has fluctuated between 30 min and 3 h [36]. In this study, a reaction time of 3 h was able to complete the Fenton oxidation of the organics in the PCLC. Therefore, the reaction time was 3 h, which was suitable for the PCLC's Fenton treatment, and set at 3 h for the following experiments.

3.2. Fenton process optimization

3.2.1. Regression model equation development

Preliminary Fenton oxidation studies have shown that pH, H_2O_2, and $FeSO_4$ were the most important factors affecting the COD removal from PCLC. The low, medium and high levels of each independent variable in coded

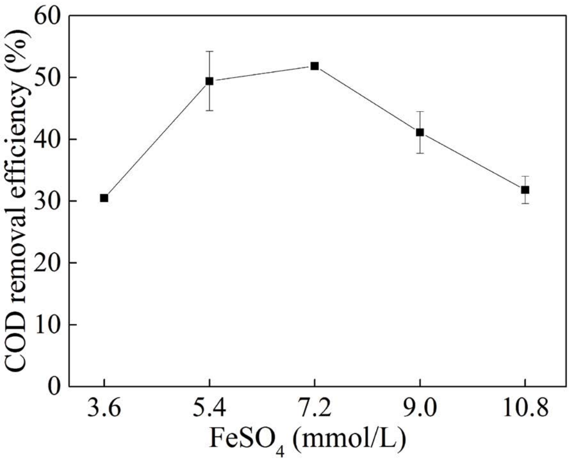

Fig. 3. Effect of $FeSO_4$ dosage on the COD removal efficiency.

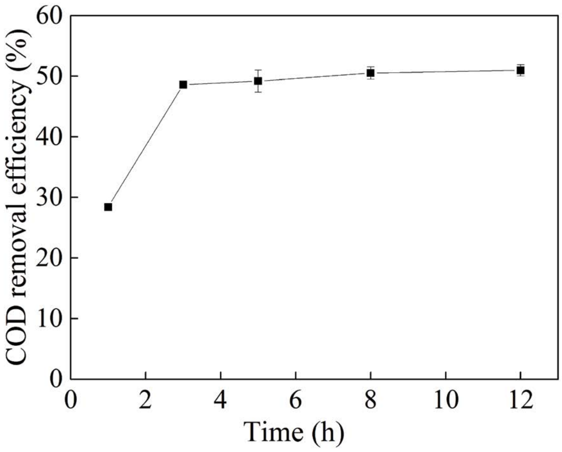

Fig. 4. Effect of reaction time on the COD removal efficiency.

form were −1, 0, +1 (Table 2). Therefore, a regression model equation was developed considering the pH, H_2O_2 dosage, and $FeSO_4$ dosage. The BBD was used to develop a correlation between the selected factors and the response values (the COD removal efficiencies).

The complete design matrix and the response values obtained from the experimental works are given in Table 2. The experimental data were calculated using Design-Expert 8.0 to obtain the regression equation for COD removal, as shown in Eq. (2):

$$\begin{aligned}\text{COD removal}(\%) &= 43.31 + 10.24(H_2O_2) \\ &+ 6.73(Fe^{2+}) - 3.62(H_2O_2)(Fe^{2+}) \\ &+ 4.60(pH)^2 - 3.98(H_2O_2)^2 - 4.79(Fe^{2+})^2 \end{aligned} \quad (2)$$

It is clear from Eq. (2) that the removal efficiency of COD was linear and also quadratic with respect to pH, H_2O_2, and Fe^{2+}. This indicated an interaction amongst these parameters for COD removal.

3.2.2. Analysis of variance study

The results of the ANOVA are given in Table 3 to evaluate the combined impact of Fenton oxidation variables (including dosages of H_2O_2 and Fe^{2+} and pH) on the COD removal. Significance of the model terms are indicated by values of "Prob. > *F*" < 0.0500 (significant) and >0.1000 (not significant), respectively. The model *F*-value of 20.10 and *p*-value of 0.0003 implied that the model was significant. In the pH range of 2–4, for COD removal rate, the doses of Fe^{2+} and H_2O_2, H_2O_2-to-Fe^{2+}, pH-to-pH, H_2O_2-to-H_2O_2, and Fe^{2+}-to-Fe^{2+} were the significant model terms that affected the COD removal. Among all the independent variables, the dosage of H_2O_2 had the greatest effect on the COD removal efficiency ($p < 0.0001$). In addition, the lack of fit with *F*-value of 0.32 was not significant relative to the pure error.

The statistical values from the ANOVA for the regression model are shown in Table 4. The R^2 value of 0.9627 indicated that the model could fit at least 96.27% of the variability in the experimental COD removal efficiencies. The signal-to-noise ratio of 19.79 (>4) implied an acceptable signal. The CV of 7.14% (<10%) [37] showed that the model had good reproducibility and accuracy. Overall, the ANOVA analysis presented satisfaction of the model in fitting COD removal.

Within the experimental design, the contour plots and three-dimensional response surfaces can be used to analyze the interactions among independent variables and responses. The circular and elliptical contours indicate insignificant and significant interaction effects between the variables, respectively [38]. The contour and response surface plots are presented in Fig. 5. Fig. 5a shows that in the pH range of 2–4, changes in the H_2O_2 dose had a significant impact on the COD removal, which increased with the increasing H_2O_2 dosage. However, pH exhibited an impact on the COD removal efficiency only at a high H_2O_2 dosage. As shown in Fig. 5c, positive interaction effects between H_2O_2 and Fe^{2+} on the COD removal were found. In the tested range of the H_2O_2 and Fe^{2+} dosage, increasing their dosage improved the COD removal efficiency. The results of ANOVA also confirmed that H_2O_2 dosage was the key factor affecting the COD removal. Fig. 5e indicates that the change in Fe^{2+} dosage resulted in a limited change in the COD removal rate in the pH range of 2–4. Fig. 5b clearly indicates that the highest COD removal efficiency of 57.40% could be achieved by adding 0.7 mol/L of H_2O_2 and

Table 2
Experimental conditions and results for the BBD

Run	Coded values			Un-coded values			Response
	pH	H_2O_2	$FeSO_4$	pH	H_2O_2 (mol/L)	$FeSO_4$ (mmol/L)	COD removal efficiency (%)
1	0	0	0	3	0.4	7.2	40.24
2	0	–1	–1	3	0.1	3.6	11.24
3	0	1	1	3	0.7	10.8	50.59
4	0	0	0	3	0.4	7.2	41.42
5	–1	0	–1	2	0.4	3.6	39.05
6	0	0	0	3	0.4	7.2	46.75
7	1	0	1	4	0.4	10.8	43.49
8	1	–1	0	4	0.1	7.2	34.91
9	0	–1	1	3	0.1	10.8	35.50
10	0	0	0	3	0.4	7.2	43.20
11	–1	–1	0	2	0.1	7.2	34.32
12	1	0	–1	4	0.4	3.6	37.28
13	–1	1	0	2	0.7	7.2	57.40
14	1	1	0	4	0.7	7.2	49.11
15	0	0	0	3	0.4	7.2	44.97
16	–1	0	1	2	0.4	10.8	52.66
17	0	1	–1	3	0.7	3.6	40.83

Table 3
ANOVA results for the COD removal efficiency

Source	Sum of squares	df	Mean square	F-value	p-value Prob. > F	Significance level
Model	1,575.28	9	175.03	20.10	0.0003	Highly significant
X_1-pH	43.43	1	43.43	4.99	0.0607	Not significant
X_2-H_2O_2	839.53	1	839.53	96.40	<0.0001	Highly significant
X_3-Fe^{2+}	362.43	1	362.43	41.62	0.0003	Highly significant
X_1X_2	19.69	1	19.69	2.26	0.1763	Not significant
X_1X_3	13.68	1	13.68	1.57	0.2504	Not significant
X_2X_3	52.54	1	52.54	6.03	0.0437	Significant
X_1^2	89.12	1	89.12	10.23	0.0151	Significant
X_2^2	66.67	1	66.67	7.66	0.0278	Significant
X_3^2	96.72	1	96.72	11.11	0.0125	Significant
Residual	60.96	7	8.71			
Lack of fit	33.37	3	11.12	1.61	0.3200	Not significant
Pure error	27.59	4	6.90			

Table 4
Statistical parameters from the ANOVA for the regression model

Parameter	Value
Std. Dev.	2.95
Mean	41.35
CV %	7.14
PRESS	577.05
R^2	0.9627
Adj. R^2	0.9148
Pred. R^2	0.6473
Adeq. precision	19.79

7.2 mmol/L of Fe^{2+} at a pH of 2. According to the optimization of this model, the theoretical removal efficiency of COD was 60.01% with the conditions of 0.7 mol/L of H_2O_2 and 9.1 mmol/L of Fe^{2+} at a pH of 2, which was not significantly different from the highest experimental value of 57.40%. Therefore, the optimal conditions for the Fenton treatment of the PCLC were a pH of 2, H_2O_2 of 0.7 mol/L, and Fe^{2+} of 7.2 mmol/L, which were used in subsequent experiments.

In order to lighten the interpretation of the parameter effect, Pareto analysis was applied based on Eq. (3) [39,40] and the Pareto graph is presented in Fig. 6.

$$P_i = \left(\frac{b_i^2}{\sum b_i^2}\right) \times 100 \quad (i \neq 0) \tag{3}$$

where P_i is the percentage effect of each variable and their combinations, b_i is the linear, quadratic or interaction coefficients in Eq. (2).

The results of Fig. 6 suggest that H_2O_2 and Fe^{2+} variables have percentage effects of 47% and 20% respectively, which produce the main effect on oxidation efficiency. The interaction effect of Fenton oxidation parameters was very limited and negligible which can facilitate the control of the process.

3.3. Organics removal analysis

When COD removal was optimal, the TOC, UV_{254} and CN removal efficiencies were 53.47%, 64.59% and 83.03%, respectively. In addition, the Fenton oxidation improved the BOD_5/COD ratio from 0.13 to 0.26, thus increasing the biodegradability of PCLC and providing the possibility for subsequent biological treatment.

The absorbance in the UV-Vis range is determined by the content of organics containing conjugated double bonds, as well as the complexity and aromatic degree of organic matter [41]. Therefore, the concentration and degradation of organic matter during wastewater treatment are usually characterized by UV-Vis absorbance spectra [42]. The UV-Vis scanning spectra (200–400 nm) of the PCLC and Fenton effluent are given in Fig. 7. The patterns of the PCLC and Fenton effluent were similar; they showed a light-absorbing peak at approximately 230 nm, while the absorbance continuously decreased in the 230–400 nm range. The Fenton treatment resulted in a significant decrease in absorbance in the approximate range of 250–300 nm, while the decrease was limited in the other ranges. The change in absorbance was consistent with the results of high UV_{254} removal. Specific absorbance can also be used to characterize the organic matter in wastewater. The ratio of E_{250} to E_{365} ($E_{250/365}$) and the ratio of E_{300} to E_{400} ($E_{300/400}$) can be employed to analyze the molecular weight and condensation degree of organic matter, respectively [41]. Changes in the integral area from 226 to 400 nm ($A_{226–400}$) indicate variations in the concentrations of organics containing benzene ring [43]. After Fenton oxidation, $E_{250/365}$, $E_{300/400}$, and $A_{226–400}$ decreased from 6.844 to 5.667, from 8.278 to 5.556, and from 110.1 to 84.48, respectively, thereby suggesting that the molecular weight of organic matter, condensation degree, and content of benzene ring substances all decreased. These results indicated that the Fenton oxidation significantly reduced the aromatic degree and complexity of coagulation-resistant organics in the PCLC.

FT-IR and EEM spectroscopies were employed to understand the removal mechanisms of organic pollutants

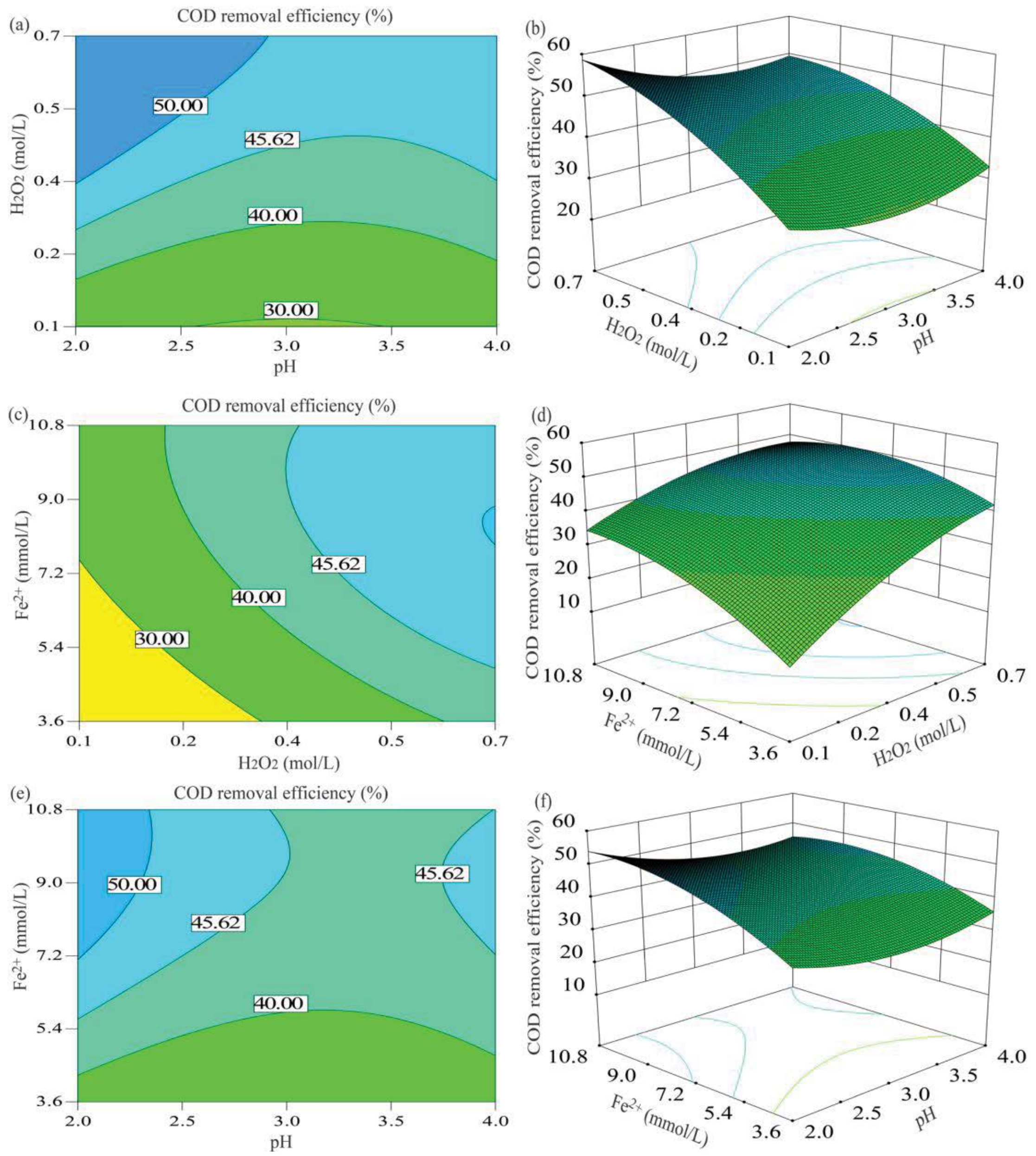

Fig. 5. Contour (a, c, and e) and response surface (b, d, and f) plots of the chemical oxygen demand (COD) removal efficiency as a function of pH and the H_2O_2 dosage at a fixed Fe^{2+} dosage (7.2 mmol/L), H_2O_2 and Fe^{2+} dosages at a fixed pH (3), and pH and Fe^{2+} dosage at a fixed H_2O_2 dosage (0.4 mol/L), respectively.

during Fenton oxidation under optimal experimental conditions. The interpretation of the absorption band was referenced in the literature [44]. The FT-IR spectra of the PCLC and Fenton effluent are shown in Fig. 8. The band at around 3,400 cm^{-1} was attributed to OH groups. The bands at approximately 1,640 cm^{-1} were attributed to the aromatic C=O stretching vibrations. The intensities of the peaks for the Fenton effluent were weaker than that for the PCLC, thereby indicating degradation of organics. The band at 1,138 cm^{-1} was closely related to C–O stretching of phenols, esters, and ethers. The intensity for the Fenton effluent was stronger than that for the PCLC, which may suggest that large molecules had been converted to smaller molecules by $HO^{•}$ oxidation. Similar results were also obtained by Xu et al. [20]. It was confirmed that some organic matter was degraded during Fenton oxidation.

The EEM fluorescence spectra of the PCLC and Fenton effluent are shown in Fig. 9. There was a considerable reduction in fluorescence intensities for the Fenton effluent, indicating that the organic matter was effectively degraded by the Fenton oxidation. The results also confirmed the previous analysis of the spectrophotometric scanning spectra. The EEM spectra of the PCLC (Fig. 9a) showed dominant responses for fulvic acid ($\lambda_{EX}/\lambda_{EM}$ = (220–250)/(380–480)) and weak responses for humic acid ($\lambda_{EX}/\lambda_{EM}$ = (325–395)/(390–500)) [45], which showed that the recalcitrant organics in the PCLC consisted mainly of fulvic acid owing to the removal of more humic acid by preliminary coagulation [9]. Fig. 9b shows that fulvic acid was removed in higher concentrations by the Fenton treatment than humic acid based on the reduction in fluorescence intensities. Teng et al. [46] also reported that fulvic-like components are preferentially oxidized by the Fenton process compared with humic-like components in LC. Thus, there may be a synergistic effect between coagulation and Fenton oxidation in the removal of the refractory organics from LC.

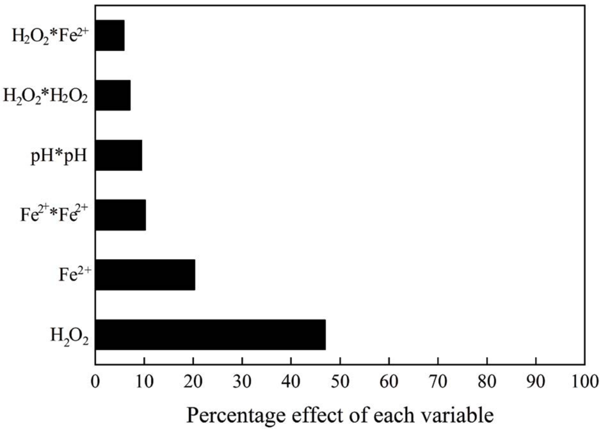

Fig. 6. Pareto chart of coagulation for the percentage effect of each variable and their combinations.

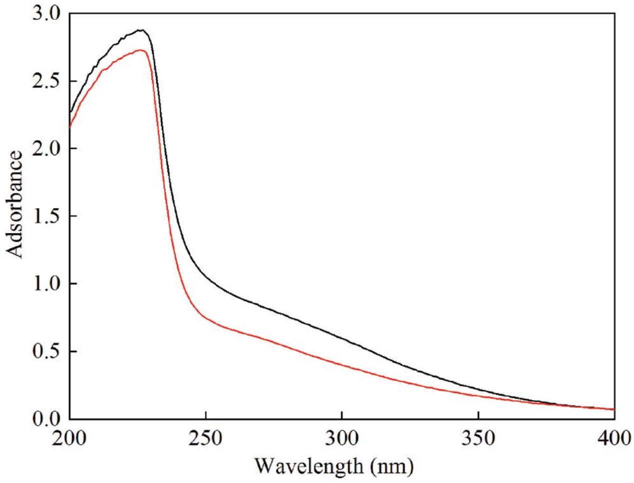

Fig. 7. Spectrophotometric analysis of the PCLC (black) and Fenton effluent (red).

4. Conclusions

In this study, batch experiments for the removal of recalcitrant organics from the PCLC using the Fenton process were carried out and optimized using RSM. The effects of variables of pH, H_2O_2 dosage and Fe^{2+} dosage on the COD removal were analyzed. The ANOVA showed that RSM can be a useful tool for the optimization of the Fenton process. The obtained model was statistically significant with R^2 value of 0.9627. The H_2O_2 and Fe^{2+} dosages produced

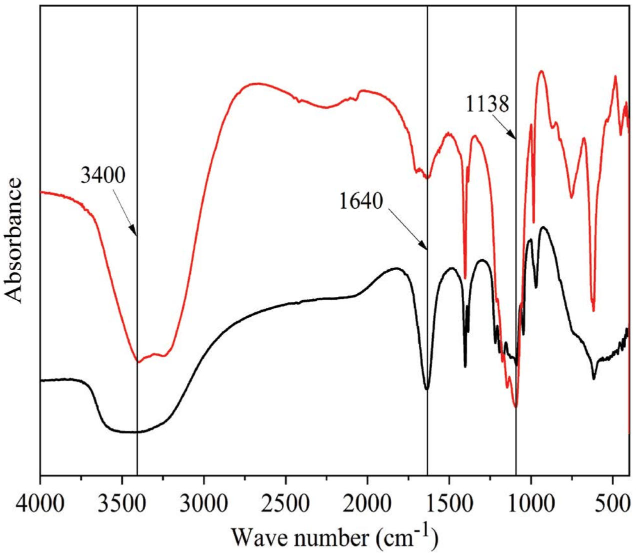

Fig. 8. Fourier transform infrared analysis of the PCLC (black) and Fenton effluent (red).

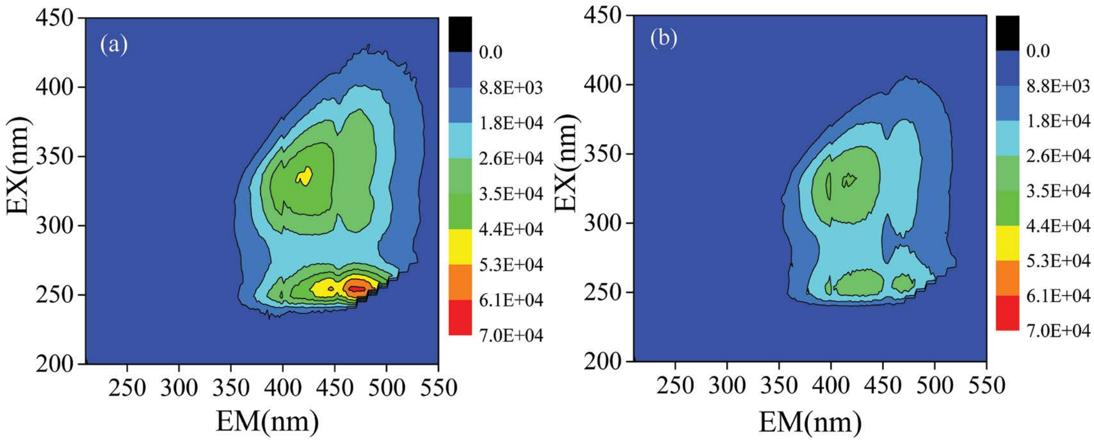

Fig. 9. Excitation-emission matrix spectra of the PCLC (a) and Fenton effluent (b).

the main effect on COD removal which had percentage effects of 47% and 20%, respectively, while the influence of pH (2–4) was not significant. The optimal conditions were obtained at a pH of 2, H_2O_2 dosage of 0.7 mol/L, and Fe^{2+} dosage of 7.2 mmol/L realizing 57.40% COD, 53.47% TOC, 83.03% CN and 64.59% UV_{254} removal, respectively. Thus, the COD concentration in the PCLC was reduced from 676 to 288 mg/L. Moreover, Fenton treatment significantly reduced the complexity and aromatic degree of coagulation-resistant organics in the PCLC and increased the ratio of BOD_5/COD from 0.13 to 0.26, improving the biodegradability of the PCLC. The PCLC mainly contained fulvic acid and humic acid, which were effectively removed by the Fenton oxidation. The PCLC treated by Fenton is suitable for possible subsequent biological treatment which can be considered for the removal of the remaining Fenton-resistant organics from the concentrate.

Acknowledgments

The authors acknowledge the financial support provided by the National Project of Training Programs of Innovation and Entrepreneurship for Undergraduates of China (Grant No. 201810448038).

References

[1] M. Qiao, X. Zhao, X. Wei, Characterization and treatment of landfill leachate membrane concentrate by Fe^{2+}/NaClO combined with advanced oxidation processes, Sci. Rep., 8 (2018) 12525, doi: 10.1038/s41598-018-30917-5.

[2] H. Wang, X. Li, Z. Hao, Y. Sun, Y. Wang, W. Li, Y. Tsang, Transformation of dissolved organic matter in concentrated leachate from nanofiltration during ozone-based oxidation processes (O_3, O_3/H_2O_2 and O_3/UV), J. Environ. Manage., 191 (2017) 244–251.

[3] H. Wang, Y. Wang, X. Li, Y. Sun, H. Wu, D. Chen, Removal of humic substances from reverse osmosis (RO) and nanofiltration (NF) concentrated leachate using continuously ozone generation-reaction treatment equipment, Waste Manage., 56 (2016) 271–279.

[4] R. He, B. Tian, Q. Zhang, H. Zhang, Effect of Fenton oxidation on biodegradability, biotoxicity and dissolved organic matter distribution of concentrated landfill leachate derived from a membrane process, Waste Manage., 38 (2015) 232–239.

[5] M. Saleem, A. Spagni, L. Alibardi, A. Bertucco, M.C. Lavagnolo, Assessment of dynamic membrane filtration for biological treatment of old landfill leachate, J. Environ. Manage., 213 (2018) 27–35.

[6] P.S. Calabrò, E. Gentili, C. Meoni, S. Orsi, D. Komilis, Effect of the recirculation of a reverse osmosis concentrate on leachate generation: a case study in an Italian landfill, Waste Manage., 76 (2018) 643–651.

[7] J. Hendrych, R. Hejralová, J. Kroužek, P. Špaček, J. Sobek, Stabilisation/solidification of landfill leachate concentrate and its residue obtained by partial evaporation, Waste Manage., 95 (2019) 560–568.

[8] B. Yang, J. Yang, H. Yang, Y. Liu, X. Li, Q. Wang, X. Pan, Co-bioevaporation treatment of concentrated landfill leachate with addition of food waste, Biochem. Eng. J., 130 (2018) 76–82.

[9] Y. Long, J. Xu, D. Shen, Y. Du, H. Feng, Effective removal of contaminants in landfill leachate membrane concentrates by coagulation, Chemosphere, 167 (2017) 512–519.

[10] E. Kattel, M. Trapido, N. Dulova, Treatment of landfill leachate by continuously reused ferric oxyhydroxide sludge-activated hydrogen peroxide, Chem. Eng. J., 304 (2016) 646–654.

[11] S.Y. Guvenc, G. Varank, Degradation of refractory organics in concentrated leachate by the Fenton process: central composite design for process optimization, Front. Environ. Sci. Eng., 2 (2021), doi: 10.1007/s11783-020-1294-1.

[12] A. Zhang, Z. Gu, W. Chen, Q. Li, G. Jiang, Removal of refractory organic pollutants in reverse-osmosis concentrated leachate by Microwave–Fenton process, Environ. Sci. Pollut. Res., 25 (2018) 28907–28916.

[13] J. Tejera, D. Hermosilla, R. Miranda, A. Gascó, V. Alonso, C. Negro, Á. Blanco, Assessing an integral treatment for landfill leachate reverse osmosis concentrate, Catalysts, 10 (2020) 1389, doi: 10.3390/catal10121389.

[14] Y. Wang, G. Meng, M. Shan, D. Wang, Z. Bai, X. Zhou, Y. Lv, J. Bai, Treatment of high-ammonia-nitrogen landfill leachate nanofiltration concentrate using an Fe-loaded Ni-foam-based electro-Fenton cathode, J. Environ. Chem. Eng., 8 (2020) 104243, doi: 10.1016/j.jece.2020.104243.

[15] L. He, H. Chen, L. Wu, Z. Zhang, Y. Ma, J. Zhu, J. Liu, X. Yan, H. Li, L. Yang, Synergistic heat/UV activated persulfate for the treatment of nanofiltration concentrated leachate, Ecotoxicol. Environ. Saf., 208 (2021) 111522, doi: 10.1016/j.ecoenv.2020.111522.

[16] Z. Huang, Z. Gu, Y. Wang, A. Zhang, Improved oxidation of refractory organics in concentrated leachate by a Fe^{2+}-enhanced O_3/H_2O_2 process, Environ. Sci. Pollut. Res., 26 (2019) 35797–35806.

[17] Q. Wu, H. Ji, N. Wei, W. Wang, Optimization of coagulation treatment process for the removal of refractory organics from leachate concentrate, Desal. Water. Treat., 195 (2020) 128–136.

[18] L. Wei, H. Zhu, X. Mao, F. Gan, Electrochemical oxidation process combined with UV photolysis for the mineralization of nitrophenol in saline wastewater, Sep. Purif. Technol., 77 (2011) 18–25.

[19] B. Kakoi, J.W. Kaluli, P. Ndiba, G. Thiong'o, Optimization of Maerua decumbent bio-coagulant in paint industry wastewater treatment with response surface methodology, J. Cleaner Prod., 164 (2017) 1124–1134.

[20] J. Xu, Y. Long, D. Shen, H. Feng, T. Chen, Optimization of Fenton treatment process for degradation of refractory organics in pre-coagulated leachate membrane concentrates, J. Hazard. Mater., 323 (2017) 674–680.

[21] H. Zhang, H.J. Choi, C.P. Huang, Optimization of Fenton process for the treatment of landfill leachate, J. Hazard. Mater., 125 (2005) 166–174.

[22] APHA, Standard Methods for the Examination of Water and Wastewater, 21st ed., American Public Health Association, Washington, DC, 2005.

[23] C. Tizaoui, L. Bouselmi, L. Mansouri, A. Ghrabi, Landfill leachate treatment with ozone and ozone/hydrogen peroxide systems, J. Hazard. Mater., 140 (2007) 316–324.

[24] B. Lai, H. Qin, X. Zhou, C. Pang, J. Xu, Y. Lian, S. Zhang, J. Zhou, Rapid detection of the degradation of the typical pollutants from ABS wastewater using Fourier transform infrared spectroscopy, Acta Opt. Sin., 2 (2011) 268–273.

[25] A. Baker, D. Ward, S.H. Lieten, R. Periera, E.C. Simpson, M. Slater, Measurement of protein-like fluorescence in river and wastewater using a handled spectrophotometer, Water Res., 38 (2004) 2934–2938.

[26] G. Wang, G. Lu, P. Yin, L. Zhao, Q. Yu, Genotoxicity assessment of membrane concentrates of landfill leachate treated with Fenton reagent and UV-Fenton reagent using human hepatoma cell line, J. Hazard. Mater., 307 (2016) 154–162.

[27] I. Gulkaya, G.A. Surucu, F.B. Dliek, Importance of H_2O_2/Fe^{2+} radio in Fenton's treatment of a carpet dyeing wastewater, J. Hazard. Mater., 136 (2006) 763–769.

[28] G.V. Buxton, C.L. Greenstock, W.P. Helman, A.B. Ross, Critical review of rate constants for reactions of hydrated electrons, hydrogen-atoms and hydroxyl radicals ($^{\bullet}OH/^{\bullet}O^{-}$) in aqueous-solution, J. Phys. Chem., 17 (1988) 513–886.

[29] C. Pulgarin, J. Kiwi, Overview on photocatalytic and electrocatalytic pretreatment of industrial non-biodegradable pollutants and pesticides, Chimia, 50 (1996) 50–55.

[30] S. Giannakis, K.A. Lin, F. Ghanbari, A review of the recent advances on the treatment of industrial wastewaters by Sulfate

Radical-based Advanced Oxidation Processes (SR-AOPs), Chem. Eng. J., 406 (2021) 127083, doi: 10.1016/j.cej.2020.127083.

[31] J. Kiwi, C. Pulgarin, P. Peringer, M. Gratzel, Beneficial effects of homogeneous photo-Fenton pretreatment upon the biodegradation of anthraquinone sulfonate in waste-water treatment, Appl. Catal., B, 3 (1993) 85–99.

[32] C.L. Hsueh, Y. Huang, C. Wang, C. Chen, Photoassisted Fenton removal of nonbiodegradable azo-dye (Reactive Black 5) over a novel supported iron oxide catalyst at neutral pH, J. Mol. Catal. A. Chem., 245 (2006) 78–86.

[33] A. Eslami, F. Mehdipour, K.A. Lin, H.S. Maleksari, F. Mirzaei, F. Ghanbari, Sono-photo activation of percarbonate for the degradation of organic dye: the effect of water matrix and identification of by-products, J. Water Process Eng., 33 (2020) 100998, doi: 10.1016/j.jwpe.2019.100998.

[34] W. Tang, C. Huang, Stoichiometry of Fenton's reagent in the oxidation of chlorinated aliphatic organic pollutants, Environ. Technol., 18 (1997) 13–23.

[35] A.G. Gutierrez-Mata, S. Velazquez-Martínez, A. Álvarez-Gallegos, M. Ahmadi, J.A. Hernández-Pérez, F. Ghanbari, S. Silva-Martínez, Recent overview of solar photocatalysis and solar photo-Fenton processes for wastewater treatment, Int. J. Photoenergy, 2017 (2017) 8528063, doi: 10.1155/2017/8528063.

[36] M. Ahmadian, S. Reshadat, N. Yousefi, S.H. Mirhossieni, M.R. Zare, S.R. Ghasemi, N.R. Gilan, R. Khamutian, A. Fatehizadeh, Municipal leachate treatment by Fenton process: effect of some variable and kinetics, J. Environ. Public Health, 3 (2013) 169682, doi: 10.1155/2013/169682.

[37] G. Varank, S.Y. Guvenc, K. Dincer, A. Demir, Concentrated leachate treatment by electro-Fenton and electro-persulfate processes using central composite design, Int. J. Environ. Res., 14 (2020) 439–461.

[38] M. Rajasimman, P. Karthic, Application of response surface methodology for the extraction of chromium(VI) by emulsion liquid membrane, J. Taiwan Inst. Chem. Eng., 41 (2010) 105–110.

[39] M. Moradi, F. Ghanbari, E. Minaee Tabrizi, Removal of acid yellow 36 using Box–Behnken designed photoelectro-Fenton: a study on removal mechanisms, Toxicol. Environ. Chem., 97 (2015) 700–709.

[40] M. Ahmadi, F. Ghanbari, S. Madihi-Bidgoli, Photoperoxi-coagulation using activated carbon fiber cathode as an efficient method for benzotriazole removal from aqueous solutions: modeling, optimization and mechanism, J. Photochem. Photobiol., A, 322 (2016) 85–94.

[41] S.S. Kavurmaci, M. Bekbolet, Specific UV-vis absorbance changes of humic acid in the presence of clay particles during photocatalytic oxidation, Desal. Water. Treat., 52 (2014) 1903–1910.

[42] X. Guo, B. Xi, H. Yu, W. Ma, X. He, The structure and origin of dissolved organic matter studied by UV-Vis spectroscopy and fluorescence spectroscopy in lake in arid and semi-arid region, Water Sci. Technol., 63 (2011) 1010–1017.

[43] F.J. Rodríguez, P. Schlenger, M. Garcíavalverde, Monitoring changes in the structure and properties of humic substances following ozonation using UV–Vis, FT-IR and ^{1}H NMR techniques, Sci. Total Environ., 541 (2016) 623–637.

[44] V. Kanokkantapong, T. Marhaba, B. Panyapinyophol, P. Pavasant, FT-IR evaluation of functional groups involved in the formation of haloacetic acids during the chlorination of raw water, J. Hazard. Mater., 136 (2006) 188–196.

[45] W. Chen, P. Westerhoff, J.A. Leenheer, K. Booksh, Fluorescence excitation-emission matrix regional integration to quantify spectra for dissolved organic matter, Environ. Sci. Technol., 37 (2003) 5701–5710.

[46] C. Teng, K. Zhou, Z. Zhang, C. Peng, W. Chen, Elucidating the structural variation of membrane concentrated landfill leachate during Fenton oxidation process using spectroscopic analyses, Environ. Pollut., 256 (2020) 113467, doi: 10.1016/j.envpol.2019.113467.